Power Electronic Systems
Laboratory

Transactions on IET Power Electronics, Vol. 7, Issue 4, February 2013

Three-Phase Rectifiers with Suboptimal Current Injection and Improved Efficiency

M. Darijevic,
M. Jankovic,
P. Pejovic,
J. W. Kolar,
Y. Nishida

Eidgenössische Technische Hochschule Zürich
Swiss Federal Institute of Technology Zurich

Published in IET Power Electronics
Received on 26th February 2013
Revised on 18th October 2013
Accepted on 20th December 2013
doi: 10.1049/iet-pel.2013.0145

ISSN 1755-4535

Three-phase rectifiers with suboptimal current injection and improved efficiency

Milan Darijević[1], Marija Janković[1], Predrag Pejović[1], Johann Walter Kolar[2], Yasuyuki Nishida[3]

[1]*Faculty of Electrical Engineering, University of Belgrade, Belgrade 11120, Serbia*
[2]*Swiss Federal Institute of Technology (ETH) Zürich, Zürich 8092, Switzerland*
[3]*Chiba Institute of Technology, Chiba 275-0016, Japan*
E-mail: peja@etf.rs

Abstract: Three-phase diode bridge rectifiers that apply suboptimal current injection and active resistance emulation are analysed. Two types of current injection devices (CIDs) are in the focus, and rectifiers with each CID are analysed for two cases of active resistance emulation: one that applies low-frequency filtering of the emulator output, and another that does not. Models that cover both continuous and discontinuous conduction mode are developed. To minimise the input current total harmonic distortion (THD), optimisation is performed, showing that in each case the THD is about the same when the emulated resistance takes its optimal value. The results are experimentally verified on a 1.5 kW rectifier.

1 Introduction

Three-phase diode bridge rectifiers are the simplest off-the-shelf solution for AC to DC conversion in medium- and high-power industrial applications [1]. Since they are characterised by excellent efficiency, almost unity power factor and simple implementation, circuits based on three-phase diode bridges have been used in various applications, such as forming DC bus voltages for machine drives [2, 3], uninterruptible power supplies systems for telecommunication facilities and other applications where unidirectional power flow is needed [4]. Unfortunately, input currents of the rectifier in its basic configuration are highly polluted with higher order harmonics. As a consequence, total harmonic distortion (THD) of the input currents for the rectifier with an inductive load is about 30%, which does not meet the standards for medium and high power applications [5].

Several solutions to this problem were proposed. Some of them are based on multi-pulse rectifiers [6], being very reliable for multi-level inverter DC bus [3]. In the case of a capacitive load, that is, the rectifier with impressed output voltage, where the bridge diodes operate deeply in the discontinuous conduction mode (DCM), harmonic reduction methods are based on semi-controlled rectifiers with high-frequency switching as the Vienna rectifier [1], or some hybrid solutions [7, 8].

For the diode rectifiers with impressed output current or with constant power load, a family of efficient solutions to reduce the mains pollution applies the current injection principle [9]. This paper introduces novel solutions to improve the efficiency of the current injection method, which was the main obstacle for wider application.

Current injection principle is shown in Fig. 1. The current injection network (CIN) is applied to generate a current on the basis of the voltage ripple at the rectifier output terminals, caused by the six-pulse switching. This current is directed towards the rectifier inputs by the current injection device (CID) and injected at the rectifier input to reduce the mains current harmonic content.

The effectiveness of current injection mainly depends on CIN structure. Theoretically, the optimal current injection [10] leads to the input current THD equal to zero. The drawback of this solution is relatively complex CIN. By modifying the CIN in comparison to [10], it is possible to simplify the system on the price of slightly increased THD [9], which corresponds to suboptimal current injection. In this case, injection of odd current harmonics is only applied, which simplifies CIN. The same idea can be applied to the 12-pulse diode rectifier [11], which does not require CID. In the case of suboptimal current injection, the input current THD is kept below 5%, which is the limit set by [5]. This paper is focused on improving the efficiency of suboptimal current injection, which seems to be a suitable solution for industrial applications, due to the circuit simplicity, performance and cost.

Both CIN and CID could be realised by using passive components only. The drawback is about 8% lower efficiency than in the initial rectifier [9], since significant amount of power is dissipated on the CIN resistors. To reduce the losses, several topologies for passive resistance emulation, such as current loaded and voltage loaded resistance emulator, are shown in [9], but they require finely tuned resonant circuitry. Besides reducing the efficiency, an additional problem introduced by resistors is a requirement to adjust their resistance according to the rectifier load

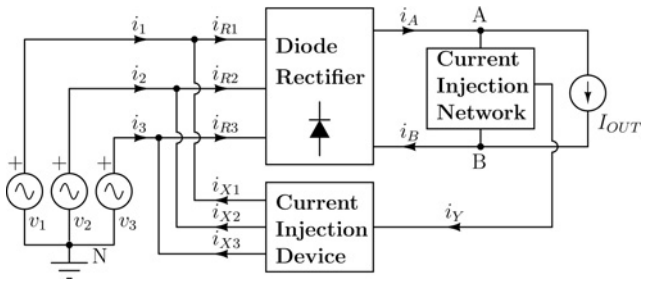

Fig. 1 *Rectifier that applies current injection method*

current. Obviously, there are strong motives to avoid the application of resistors.

A method to avoid the drawbacks associated with the use of resistors is to use active resistance emulation introduced in [12]. An active resistance emulation circuit that applies a concept of loss-free resistor [13] is addressed in this paper. The emulator contains a small transformer, single-phase rectifier diode bridge and a boost converter, as presented in [14]. In most of the previous research efforts, low-frequency filtering of the boost converter output current is applied, that is, the resistance emulator output current is filtered and just its DC component is supplied as a part of the load current. However, the overall rectifier efficiency, input power factor and THD of the input currents are comparable in cases when the filter is applied and when it is not [15].

CIN with active resistance emulation can be combined with different types of CID, such as magnetic CID (MCID) as presented in [15], or with switched mode CID (SCID) introduced in [16]. Structures of MCID and SCID are shown in Fig. 2. MCID could be realised in various ways [9]. One of them is based on zig-zag autotransformer (Fig. 2*a*), and it provides equal current injection in all the three phases. This is a simple solution, but it has several drawbacks:

- The power losses may be significant due to the series resistance of the windings.
- Zig-zag transformer or any other passive CID solutions are based on heavy and expensive components [9].
- Theoretically, the current should be injected to one phase at a time. Since MCID injects in all three phases equally, the rated power of the device is relatively high [9], affecting the cost and power density.

In contrast to MCID, SCID consists of three bidirectional switches that are switched at a double of the line frequency (Fig. 2*b*). Instead of injecting current in all the three phases

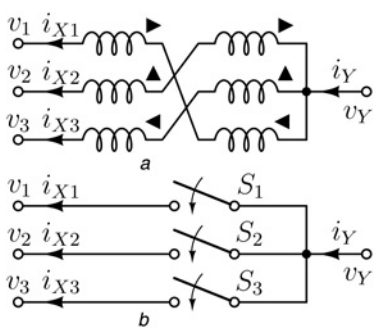

Fig. 2 *Two types of CID*

a MCID (zig-zag transformer)
b SCID with three bidirectional switches

simultaneously, SCID provides current injection in only one phase at a certain moment. The current is injected in the input phase whose voltage is neither minimal nor maximal at that time. Replacing the bulky transformer of MCID with SCID reduces the converter size and weight. Similar replacement of MCID with SCID in a thyristor rectifier is presented in [17]. Some hybrid solutions for lowering the input current THD use SCID as well [8, 18, 19]. In [8], SCID is used for high-power rectifier, together with CIN based on bidirectional multi-level cell. Similar realisation based on both CID and CIN in switched mode is presented in [18, 19]. Significant difference in performance presented in [18, 19] is in part a consequence of a different control of the SCID switches, which is discussed in Section 4.

The application of SCID reduces the injected current amplitude three times, since the current is injected in only one phase, not in three. This affects the range of the DCM operation, making it irrelevant when SCID is used.

Omitting low-frequency filtering at the resistance emulation output is another possibility to reduce the rectifier weight and size, and even to improve the efficiency. Therefore, comparison of the rectifier performance when MCID and SCID are used in combination with filtering and without filtering of resistance emulator output current is the focus of this research.

Rectifier models for each type of CID and each type of the resistance emulator output current filtering are required to perform optimisation of the emulated resistance and to compare the solutions. Besides, depending on the value of the emulated resistance and the chosen topology, the rectifier could operate either in the continuous conduction mode (CCM) or the DCM. Boundaries between the conduction modes are derived as a result of the model analysis. Numerical simulation of the rectifier with the emulated resistance as a variable parameter is performed aiming at a minimum of the input current THD. The optimal value of the emulated resistance is found, and it is shown that it might correspond either to the CCM or the DCM depending on the rectifier CID and the resistance emulator output current filtering. Simulation results confirmed the improvement in the rectifier efficiency, while the input current THD stays below 5%. The results are experimentally confirmed on 1.5 kW laboratory prototype.

2 Models

The rectifier under analysis is presented in Fig. 3. It consists of a three-phase diode bridge (D_1 to D_6), a current injection device (MCID or SCID), a current injection system (capacitor and 1:1 transformer) and a resistance emulator accompanied by an output filter. The output filter might be the one that provides both the low-frequency (multiples of the line frequency) and the high-frequency (multiples of the switching frequency) filtering, or the one that provides only the high-frequency (electromagnetic interference (EMI)) filtering. The first case is named the filtering case, whereas the second is named no filtering case, although the high-frequency EMI filter is present in this case. In the filtering case, only a DC component is provided from the resistance emulator to the load.

To analyse the rectifier with either MCID or SCID, both in the filtering and in the no filtering case, appropriate models should be derived. In the analysis, both CCM and DCM might be of interest, and the models should cover for the modes expected to occur.

doi: 10.1049/iet-pel.2013.0145

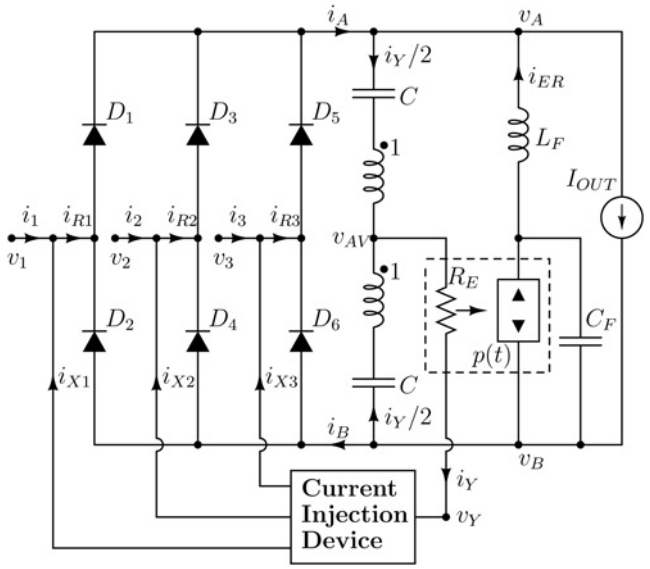

Fig. 3 *Rectifier circuit for model derivation; resistance emulation is presented as loss-free resistor in dashed rectangle*

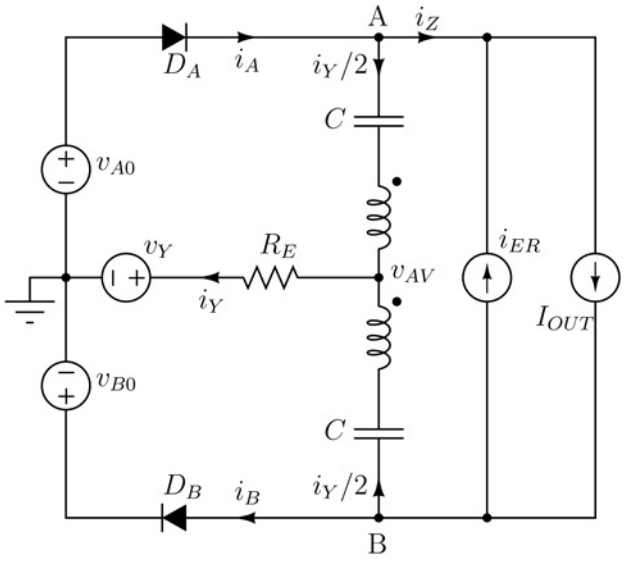

Fig. 4 *Equivalent circuit of the rectifier*

In the analysis, it is assumed that the rectifier is supplied by a balanced undistorted three-phase voltage system

$$v_k = V_m \cos\left(2\pi ft - (k-1)\frac{2\pi}{3}\right) \tag{1}$$

where V_m is the amplitude and f is the frequency of the phase voltages, while $k \in \{1, 2, 3\}$ is the phase index. Let the waveforms v_{A0} and v_{B0} be defined as

$$v_{A0} = \max(v_1, v_2, v_3) \tag{2}$$

and

$$v_{B0} = \min(v_1, v_2, v_3) \tag{3}$$

In addition, let the waveform v_{AV} be defined as

$$v_{AV} = \frac{v_A + v_B}{2} \tag{4}$$

regardless of the conduction states of the diodes. As labelled in Fig. 3, v_A and v_B are the voltages at the diode bridge output terminals. All the voltages are referred to the three-phase voltage system neutral point, labelled with N in Fig. 1. In the case the diode bridge operates in the CCM, $v_{AV} = v_{AV0}$, where v_{AV0} is defined as

$$v_{AV0} = \frac{v_{A0} + v_{B0}}{2} \tag{5}$$

To determine the input current waveforms, it is sufficient to determine the waveforms of i_A and i_B, since all other currents can be derived from these currents and the input voltages.

In order to simplify the analysis, the rectifier of Fig. 3 can be represented by the equivalent circuit of Fig. 4 [20]. In this circuit, the diode bridge is represented by D_A and D_B, the CID with the voltage source v_Y, the CIN is the same as in Fig. 3, while the resistance emulation circuit is represented by R_E and i_{ER}. Since i_{ER} depends on the filtering at the resistance emulator output, its waveform will be derived separately depending on the analysed filtering case. On the other hand, i_Y is determined by

$$i_Y = \frac{v_{AV} - v_Y}{R_E} \tag{6}$$

regardless of the operating modes.

In the CCM, diodes D_A and D_B conduct during the whole period, resulting in $v_A = v_{A0}$ and $v_B = v_{B0}$. When the rectifier operates in the DCM, there are time intervals in which currents i_A or i_B are equal to zero, since the corresponding diode (D_A or D_B) is reverse-biased. In these intervals, v_A or v_B are different from v_{A0} or v_{B0}, respectively.

In the case filtering of the resistance emulation output is applied, the current source i_{ER} is constant $i_{ER} = I_{ER}$, while when the filtering is omitted the current source waveform contains AC ripple at multiples of $6f$. In case MCID is used, $v_Y = 0$, while in the case of SCID is used, $v_Y = -v_{A0} - v_{B0}$, assuming the CCM.

2.1 Rectifier with MCID and low-frequency filtering of the resistance emulator output

In the case of low-frequency filtering of the resistance emulator output is applied, the diode bridge load current is effectively reduced to $I_Z = I_{OUT} - I_{ER}$. Since the MCID is used, $v_Y = 0$. Analysis of the non-linear circuit of Fig. 4 reduces to analyses of three relevant linear equivalents. The first one corresponds to the case when both of the diodes conduct, and in that case the diode bridge output terminal currents are

$$i_A = I_Z + \frac{i_Y}{2} \tag{7}$$

and

$$i_B = I_Z - \frac{i_Y}{2} \tag{8}$$

and the injected current is

$$i_Y = v_{AV0}/R_E \tag{9}$$

The above equation applies when $v_{AV0} > -2R_E I_Z$ and $v_{AV0} < 2R_E I_Z$. These conditions border the CCM and the DCM: if they are satisfied during the whole period the rectifier operates in the CCM, whereas in the opposite case it operates in the DCM.

The second linear equivalent applies in the case $v_{AV0} > 2R_E I_Z$, when the diode D_A conducts and the diode D_B does not. The voltage v_A is v_{A0}, while

$$v_B = -v_A + 4R_E I_Z \tag{10}$$

$$i_A = i_Y = 2I_Z \tag{11}$$

and

$$i_B = 0 \tag{12}$$

The third linear equivalent applies for $v_{AV0} < -2R_E I_Z$ when D_A is off and D_B conducts. In that case, $v_B = v_{B0}$, $v_A = -v_B - 4R_E I_Z$, $i_B = -i_Y = 2I_Z$ and $i_A = 0$.

To determine the waveforms of the rectifier currents, it is convenient to assume a value of I_Z, and to compute all other waveforms on the basis of I_Z. The actual output current of the rectifier is computed as $I_{OUT} = I_Z + I_{ER}$ at the end, where the resistance emulator output current is obtained from

$$I_{ER} = \langle \frac{R_E i_Y^2}{v_A - v_B} \rangle \tag{13}$$

and $\langle \cdot \rangle$ represents averaging over the line period. As derived, the DCM occurs when the amplitude of the injected current reaches $2I_Z$.

2.2 Rectifier with MCID and without low-frequency filtering of the resistance emulator output current

In this case, the resistance emulator output current i_{ER} contains both the DC and AC components. This current is determined by

$$i_{ER} = \frac{R_E i_Y^2}{v_A - v_B} \tag{14}$$

Again, since MCID is used, $v_Y = 0$, and the injected current is $i_Y = v_{AV}/R_E$.

Similar to the previously analysed case, three linear equivalent circuits are relevant, one with both D_A and D_B conducting, while in the other two one of the diodes is not conducting. When both the diodes are conducting, $v_A = v_{A0}$, $v_B = v_{B0}$, and i_A and i_B are given by

$$i_A = I_{OUT} - \frac{v_{AV0}}{R_E} \frac{v_{B0}}{v_{A0} - v_{B0}} \tag{15}$$

and

$$i_B = I_{OUT} - \frac{v_{AV0}}{R_E} \frac{v_{A0}}{v_{A0} - v_{B0}} \tag{16}$$

This applies for $i_A > 0$ and $i_B > 0$.

In the case when D_A is off and D_B is on, v_B is v_{B0}, while v_{AV} and v_A are

$$v_{AV} = 2R_E I_{OUT} \frac{v_{B0}}{-v_{B0} + 2R_E I_{OUT}} \tag{17}$$

and

$$v_A = 2v_{AV} - v_{B0} \tag{18}$$

The diode bridge terminal currents i_A and i_B are

$$i_A = 0 \tag{19}$$

and

$$i_B = -i_Y = 2I_{OUT} \frac{v_{B0}}{v_{B0} - 2R_E I_{OUT}} \tag{20}$$

This applies for $v_A > v_{A0}$.

In the case of D_A is on and D_B is off, v_A is v_{A0}, while v_{AV} and v_B are

$$v_{AV} = 2R_E I_{OUT} \frac{v_{A0}}{v_{A0} + 2R_E I_{OUT}} \tag{21}$$

and

$$v_B = 2v_{AV} - v_{A0} \tag{22}$$

The currents i_A and i_B are given by

$$i_A = i_Y = 2I_{OUT} \frac{v_{A0}}{v_{A0} + 2R_E I_{OUT}} \tag{23}$$

and

$$i_B = 0 \tag{24}$$

This applies for $v_B < v_{B0}$.

2.3 Rectifier with SCID and low-frequency filtering of the resistance emulator output current

When SCID is used, v_Y is equal to the phase voltage that is neither minimal nor maximal, and it is given by $v_Y = -v_{A0} - v_{B0} = -2v_{AV0}$. Assuming CCM and the same operating conditions as in the case when MCID was used, the rectifier with SCID has injected current equal to one-third of the injected current of the rectifier with MCID. In addition, the voltage across the emulated resistance $v_{AV0} - v_Y = 3v_{AV0}$ is three times higher. This means that emulated resistance in the case of SCID is applied is nine times higher than the corresponding emulated resistance when MCID was applied, while processed power is the same. The rectifier would enter the DCM if the injected current amplitude reaches the same value as in case of the rectifier with MCID. However, in the SCID case, the injected current is three times lower, and the CCM–DCM border is far from the region of practical interest. The optimisation results place the emulated resistance close to the CCM–DCM border in the case of MCID, but deep within the CCM region when the SCID is applied; thus, from the analysis the SCID case focuses on the CCM only. In the CCM, similarly to the case presented in Section 2.1,

doi: 10.1049/iet-pel.2013.0145

equations for currents i_A and i_B are

$$i_A = I_Z + \frac{i_Y}{2} \tag{25}$$

and

$$i_B = I_Z - \frac{i_Y}{2} \tag{26}$$

where I_Z is given by $I_Z = I_{OUT} - I_{ER}$. The injection current is $i_Y = 3v_{AV0}/R_E$. This applies for $i_A > 0$ and $i_B > 0$. The region of interest fits within these limits.

2.4 Rectifier with SCID and without low-frequency filtering of the resistance emulator output current

When low-frequency filtering of the resistance emulator output is not applied, the emulator output current i_{ER} is given by (14). Again, since SCID is used, $v_Y = -v_{A0} - v_{B0} = -2v_{AV0}$, resulting in

$$i_Y = 3\frac{v_{AV}}{R_E} \tag{27}$$

The discussion on the operating mode presented in previous subsection applies here, as well. The rectifier with SCID, when filtering of the resistance emulator output current is omitted, operates deeply in the CCM, while corresponding rectifier with the MCID operates near the CCM–DCM border. This simplifies the circuit analysis, which reduces to the linear equivalent that corresponds to the CCM. The diode bridge output terminal voltages are $v_A = v_{A0}$ and $v_B = v_{B0}$ resulting in

$$i_A = I_{OUT} - 3\frac{v_{AV0}}{R_E}\frac{2v_{B0} + v_{A0}}{v_{A0} - v_{B0}} \tag{28}$$

and

$$i_B = I_{OUT} - 3\frac{v_{AV0}}{R_E}\frac{2v_{A0} + v_{B0}}{v_{A0} - v_{B0}} \tag{29}$$

The above equations apply for $i_A > 0$ and $i_B > 0$, which is satisfied in the region of interest.

3 Optimisation

To determine the optimal emulated resistance, numerical simulation is performed using GNU Octave 3.2. The simulation is performed using the models derived for each rectifier topology. To simplify the analysis, the waveforms of i_A, i_B and i_Y are computed first, whereas the waveforms of i_1, i_2 and i_3 are constructed later, depending on the instantaneous values of the phase voltages, also used for determining the states of the switches in the SCID when applied. In order to generalise the results, normalisation is performed. All currents are normalised to $j(t) = i(t)/I_{OUT}$, while voltages are normalised to $m(t) = v(t)/V_m$. Resulting THD of the input currents is expressed in terms of normalised conductance at the resistance emulator input port, defined as $G = V_m/(R_E I_{OUT})$.

The optimisation results are presented in Table 1, for all the four cases. The optimal normalised conductance (G), with corresponding THD and recovered power (relative to the input power) are given. Results indicate that the optimal THD is achieved in DCM for the case when MCID is used and filtering at the emulator output is omitted. In the remaining three cases, the rectifier operates in CCM. In the filtering case, minimum of THD(G) is about the same and it is achieved in the same mode for the rectifier with MCID and SCID. Therefore, it is expected that the input current waveforms are the same. The only difference, as discussed in Section 2, is the nine times higher emulated resistance in the SCID case, providing nine times lower normalised conductance. These results are verified on experimental 1.5 kW prototype, as shown in Section 5.

Table 1 Optimisation results

Parameter	MCID filter	MCID no filter	SCID filter	SCID no filter
THD_{MIN}	4.01%	4.22%	4.01%	4.36%
G_{OPT}	6.62	6.5	0.735	0.705
P_{ER}/P_{IN}	8.66%	8.40%	8.66%	8.30%
mode	CCM	DCM	CCM	CCM

4 Improved control of the SCID

The control algorithm for bidirectional switches in the SCID is simple, being based on mutual comparison of the phase voltages. The control algorithm can be implemented applying three comparators and some elementary logic circuitry [16] to provide control signals presented in Fig. 5*a*. However, when the algorithm is implemented in its raw form, the input current waveforms suffer from spikes. During the experiments, it is observed that the phase currents contain spikes at the moments when the switches transfer conduction of the injected current from one to another, as shown in Fig. 5*b*. In this case, the experimentally obtained THD is 7.61% for the optimal value of G, which is not in agreement with the theoretical predictions.

The detailed analysis showed that the spikes are not a consequence of large transient times of the bidirectional switches, nor overlapping in their conduction. Instead, occurrence of the spikes in phase currents is a result of the control logic designed assuming an ideal case where there are no leakage inductances in the supply lines and the comparators do not have any offset nor delay. Leakage inductances cause the overlap phenomenon, when the rectifier diodes do not change their states instantaneously, and short circuit involved phases during the commutation intervals [21, 22]. Besides the spikes in the input currents, notches in the phase and line voltages occur during the commutation intervals.

The essence of the problem is illustrated in Fig. 6*a*. Notch in the line voltage (CH4) results in distorted reference signal that controls the switches by the algorithm proposed in [16]. This control method cannot decide the switch states when the line voltage is zero, and the decision is made by the comparator offset. If the offset is such that the state transition of the switches is late, the system enters slow diode commutation process. In that case, during the notch which coincides with the input current spike, the diode bridge input current (CH2) slowly goes to zero. The injected current (CH3) starts to flow only after the slow commutation of diodes is completed, when the comparator can initiate the state change in the SCID, since it observes voltage different than zero. In the case presented in Fig. 6*a*,

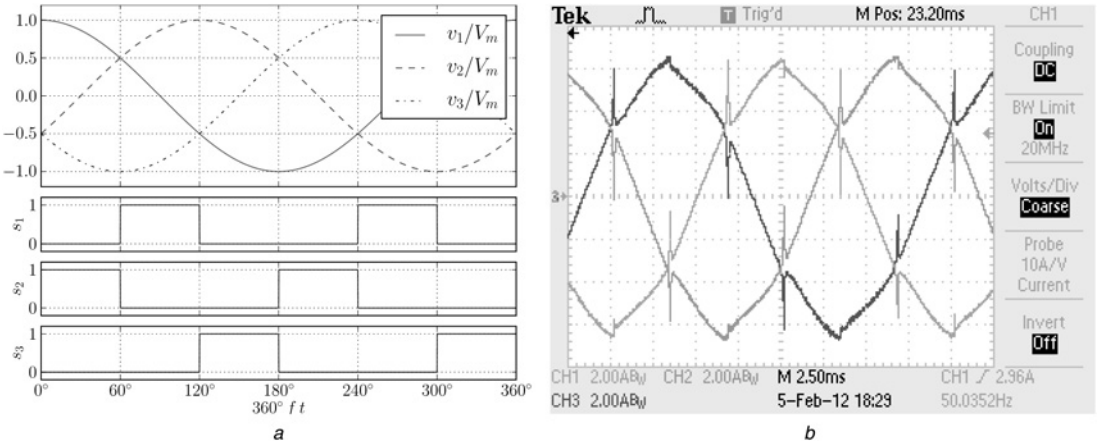

Fig. 5 *SCID control*

a Phase voltages and switch control signals
b Experimentally obtained waveforms of the phase currents for simple SCID control circuit

the phase current is rising and belated current injection caused the upward spike. In the case a phase current is falling, belated start of current injection causes a downward spike. The spikes always appear in pairs, in two phases that are involved in the commutation process.

To avoid the spikes, state transitions of the SCID switches should be initiated precisely, not allowing the slow diode commutation process to start. There are six switch commutations in the SCID per period. Precise adjustment of the commutation instants can be done by adjusting the

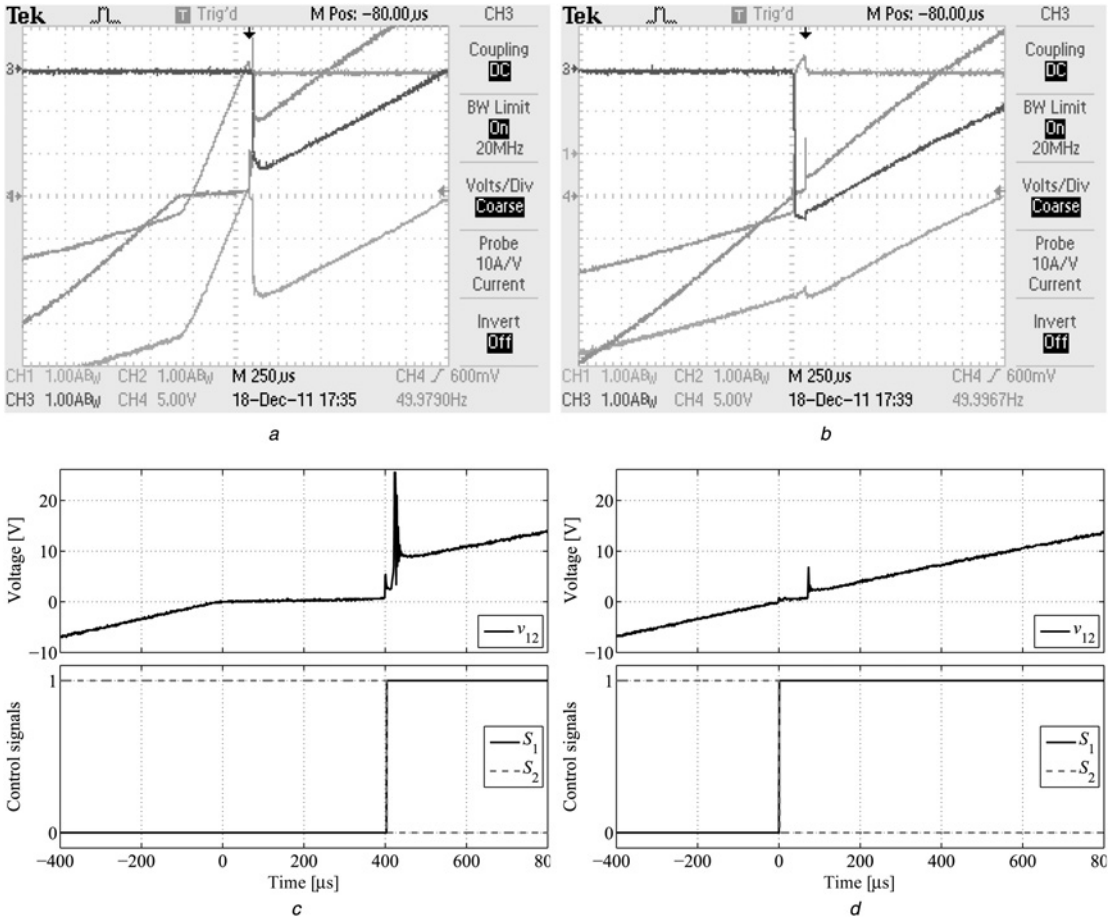

Fig. 6 *Transition zone*

Phase current i_1 (CH1, yellow trace), diode bridge input current i_{R1} (CH2, blue trace), the injected current $-i_{X1}$ (CH3, purple trace) and the line voltage $v_{12} = v_1 - v_2$ (CH4, green trace)
a Simple control
b Improved control; corresponding SCID control signals with relation to the line voltage
c Simple control
d Improved control

doi: 10.1049/iet-pel.2013.0145

comparator offset. However, the control scheme of [16] involves only three comparators and provides three degrees of freedom for the adjustment; thus, six commutation intervals cannot be tuned independently. To provide three additional degrees of freedom, another three comparators are introduced. In this manner, detection of zero crossings of all six line voltages with the corresponding offset levels, provide precise and independent tuning of all transitions. Rising edges of the comparator output voltages are decoded to initiate commutations, one transition corresponding to one commutation. In analogue implementation, this improvement involves minor increase in the controller cost. On the other hand, a digital implementation would require just a software modification.

Commutation intervals in cases of original and improved SCID control algorithm are presented in Figs. 6*a* and *b*, respectively. The SCID switching signals corresponding to the involved phases are presented in Fig. 6*d* for improved algorithm, and in Fig. 6*c* for original algorithm. The introduced offsets in SCID control provided that injection in certain phase starts before the commutation interval. The input current spike is eliminated, and the commutation process is shorter. It can be noticed that the injected current and the input current of the diode bridge fit each other very well, and that the phase voltage notch is significantly reduced.

The improved control method results in reduction of the rectifier input current THD from 7.61% to 4.25%, which is close to the theoretical expectations. The waveforms of the input currents obtained with the improved SCID control are shown in Fig. 7. The comparison of the waveforms of Figs. 5*b* and 7 shows that the spikes are completely removed from the input currents.

In previous publications, results reported in [18] contain spikes in phase currents, which likely is a consequence of the described phenomena. However, in [8, 17], spikes in phase currents are not present, which might be caused by low leakage inductance of the supply lines. In [19], the improved algorithm is implemented, although not described, since the focus of that paper is in the rectifier topology. Improvements in the SCID control were necessary to provide proper experimental verification in [19].

5 Experimental results

To verify the analytically obtained results, an experimental setup is built. This setup consists of a 1.5 kW diode rectifier, with the CIN that provides active resistance emulation and an option of low-frequency filtering of the resistance emulator output current. Two types of CID are

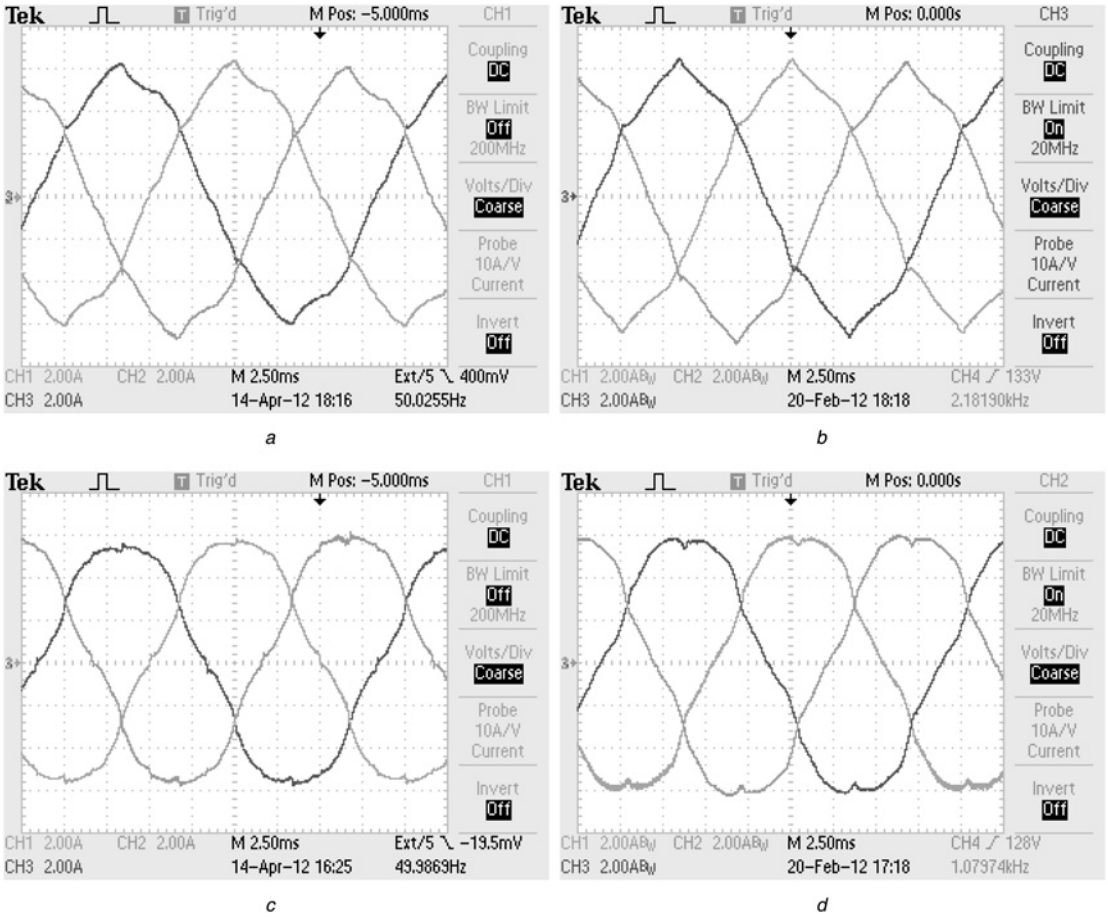

Fig. 7 *Experimentally obtained phase current waveforms*

Filtering
a MCID
b SCID
Without filtering
c MCID
d SCID

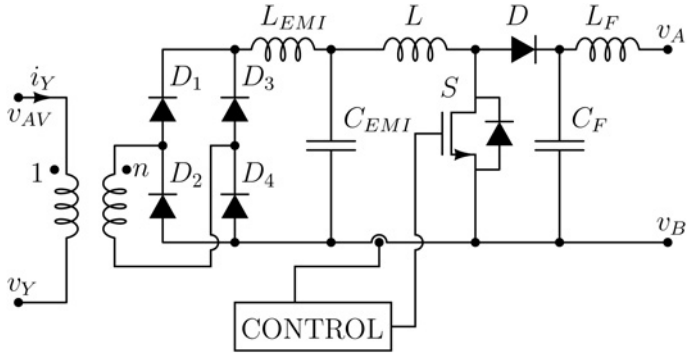

Fig. 8 *Active resistance emulator*

Table 2 Experimental results

Parameter	MCID filter	MCID no filter	SCID filter	SCID no filter
THD_{MIN}	4.43%	4.46%	4.25%	4.45%
G_{OPT}	6.56	6.19	0.72	0.69
η	96%	97%	98%	98%
PF	0.995	0.997	0.998	0.993

supported, the magnetic and the switched mode one. The rectifier is supplied by the phase voltages with $V_m = 135$ V, and $f = 50$ Hz. In all of the four cases, the output voltage was about 225 V and the output current was 5 A, resulting in the input current amplitudes of about 6 A.

The active resistance emulator is shown in Fig. 8. The boost converter is controlled applying the hysteresis window method, providing the switching frequency that varies around 70 kHz for the inductance $L = 500$ μH. Thus, light EMI filtering at the boost converter input is required ($L_{EMI} = 140$ μH and $C_{EMI} = 150$ nF). As already addressed, voltages across the emulator input port are different for MCID and SCID. Therefore, in order to avoid extreme values for the boost converter duty ratio, different turns ratio n is used for the resistance emulator input transformer depending on the CID type.

The resistance emulator output filter components L_F and C_F are 1.25 mH and 2200 μF for the low-frequency filtering case, and 70 μH and 200 μF to provide only EMI filtering in the case when low-frequency filtering is omitted. EMI filtering is mandatory, since active resistance emulator input and output currents contain high-frequency components, which are not desirable in both injected current and output current.

Dependence of the input current THD on G obtained by simulation accompanied by the experimentally obtained data is presented in Fig. 9 for both of the CID types. The results are in good agreement. The input current waveforms obtained for the optimal value of the emulated resistance are presented in Fig. 7. The waveforms are close to sinusoidal, having difference in shape depending on the filtering.

The quantitative parameters of the experimentally obtained waveforms are summarised in Table 2. Comparison of Tables 1 and 2 together with Fig. 9 indicates a good agreement of optimal emulated conductance and corresponding THD predicted by optimisation to the values obtained experimentally. THD of the supply voltages during the experiments was about 2.9%. In all of the four

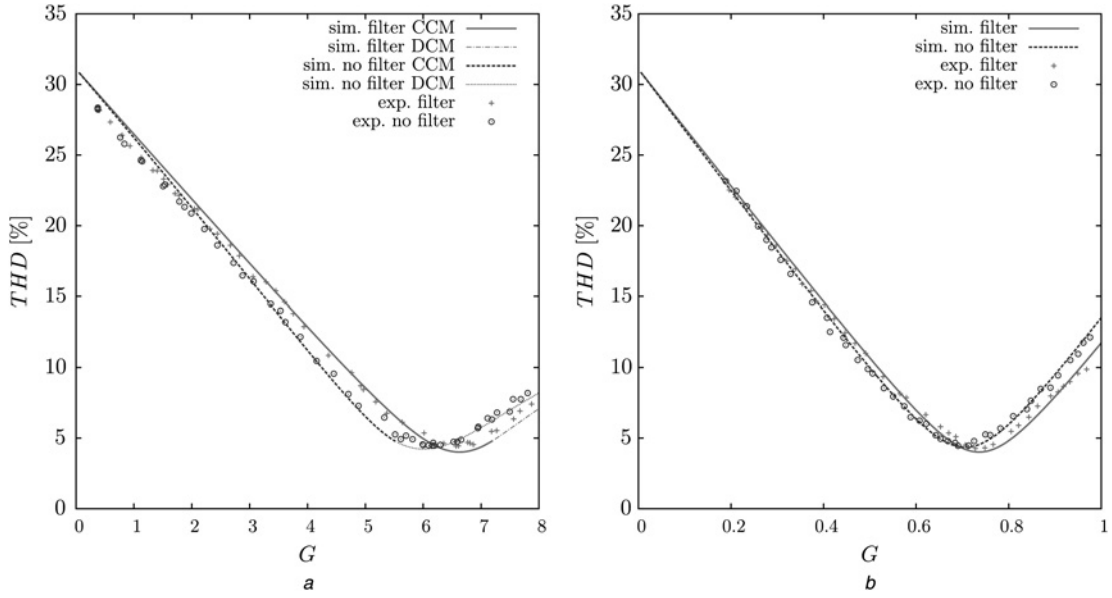

Fig. 9 *Theoretical predictions and experimental results for input current THD*

a MCID
b SCID

doi: 10.1049/iet-pel.2013.0145

Table 3 Power measurements

	MCID filter	MCID no filter	SCID filter	SCID no filter
P_{IN}, W	1226.63	1220.58	1182.40	1239.68
$P_{bridgeOUT}$, W	1129.73	1130.51	1075.24	1117.34
P_{ER}, W	50.41	63.88	68.22	73.67
P_{OUT}, W	1183.37	1203.06	1148.29	1213.58

cases, the power factor is higher than 0.99. The rectifier efficiency is better in the case SCID is applied. This is expected, since the series resistance of the MCID zig-zag transformer is about 3 Ω per phase. On the other hand, switching losses in SCID are negligible and the forward voltage drop across the switches is moderate. Filtering reduces the rectifier efficiency since the filter introduces additional losses.

To follow the power flow in all four of the analysed rectifiers, data about the rectifier input power (P_{IN}), the diode bridge output power ($P_{bridgeOUT}$), the resistance emulator output power (P_{ER}) and the output power (P_{OUT}) are given in Table 3. Measurements are performed applying a Tektronix TDS 2024 oscilloscope (8-bit resolution) and a current probe Agilent 1146 A (accuracy 3%), taking 2000 samples per fundamental period of 20 ms. The results indicate that some power, varying from about 4% to about 6% of the input power, depending on the rectifier analysed, is recovered at the rectifier output, contributing to the rectifier efficiency.

The waveforms shown in Fig. 7 indicate that choice of the CID type does not affect the input currents, while the waveforms are affected by the resistance emulator output current filtering. However, the THD values of the input currents are about the same in all of the four analysed cases.

The waveforms shown in Figs. 7*a* and *b* are slightly different, although in theory they should be the same. The difference is caused by the output current ripple, mainly consisting of the sixth harmonic with the amplitude equal to 3% of the DC value. This ripple was present in the experiments when the waveforms of Fig. 7*a* were captured, even though the filtering was applied. The difference in waveforms shown in Figs. 7*c* and *d* is expected, due to the fact that for the case without filtering, the rectifier with MCID operates in DCM at optimum point, while the rectifier with SCID operates in CCM.

6 Conclusions

In this paper, suboptimal current injection method for three-phase diode bridge rectifiers [9] is addressed. The rectifier structure is chosen to provide compromise between the rectifier complexity and performance, resulting in the input current THD values lower than 5% while the rectifier efficiency is improved from typical 92% [9] to about 98%. This is achieved by applying switched resistance emulator and a simple CIN consisting of two capacitors and a transformer.

The resistance emulator is based on a boost converter [12, 14, 15], and it is applied to improve the system efficiency by recovering the power of CIN resistor at the rectifier output. Since the rectifier is loaded with a constant current, the main implementation issue of this concept is how to process the emulator output current, whether to filter it or not. These two cases are analysed with two different types of CID. The first one is built as a passive magnetic component and provides equal currents injected to all of the input phases. The second device consists of three bidirectional switches used to select in which phase the current is injected, reducing the overall current in the current injection system by a factor of three.

Depending on the resistance emulator output current filtering and the choice of the CID, four systems are distinguished. For all of them, equivalent rectifier models are derived, using the method of equivalent circuits introduced in [20]. The models are applied to perform numerical optimisation of the emulated resistance in order to minimise the THD of the input currents. Since the rectifiers with magnetic CID tend to operate close to the DCM, the derived models cover both the CCM and the DCM in this case. For the rectifier that applies filtering, the minimum of the THD is obtained in the CCM, while in the rectifier that does not apply filtering the THD minimum is obtained in the DCM.

In the case of switched mode CID is applied, the optimum is reached in the CCM in both the cases. At the same time, the injected current is three times lower than in the case of the MCID, which lowers the component ratings, power losses and price. In the analyses, the rectifiers are treated as resistive circuits, assuming constant voltages across the capacitors of the CIN, as well as assuming ideal filtering of the resistance emulator output current when applied.

In this paper, improvements in the control of the switching CID are described, as well. Experimentally observed spikes in the input currents are focused. Detailed analysis is performed, and the cause of these spikes is found in improper timing of the switch state changes in the CID. The effect is further worsened by resulting notches in the phase voltages during the commutation of the diodes in the bridge. A simple solution to this problem is presented, based on independent timing control for all six of the switching instances per period. Simple analogue circuitry is applied to perform the control. Complete removal of the spikes is experimentally demonstrated. The results are experimentally verified on a rectifier laboratory model with the rated power of 1.5 kW. The experimental results are in good agreement with theoretical predictions, and the input current THD below 5% is achieved in all of the cases.

According to the performed analyses, as well as the experimental results, it can be concluded that for both of the CIDs filtering of the resistance emulator output current provides negligible improvement. Having in mind the drawbacks of the low-frequency filtering, such as increase in power losses, increase of the rectifier volume, weight and price, it is clear that filtering of resistance emulator output current should be omitted. Regarding efficiency, the SCID with improved control method provided superior performance in comparison to the MCID alternative.

7 References

1 Kolar, J.W., Ertl, H.: 'Status of the techniques of three-phase rectifier systems with low effects on the mains'. Proc. Int. Telecommunication Energy Conf. INTELEC, Copenhagen, Denmark, June 1999, pp. 1–16

2 Singh, B., Bhuvaneswari, G., Madishetti, S.: 'Power quality improvement in DTC based induction motor drive using Minnesota rectifier'. Proc. Int. Conf. Power and Energy Systems ICPES, Pune, India, December 2011, CD-ROM paper

3 Rodriguez, J., Bernet, S., Bin, W., Pontt, J.O., Kouro, S.: 'Multilevel voltage-source-converter topologies for industrial medium-voltage drives', *IEEE Trans. Ind. Electron.*, 2007, **54**, (6), pp. 2930–2945

4 Malinowski, M., Kazmierkowski, M.P.: 'The industrial electronics handbook: Power electronics and motor drives' (CRC Press, 2011, 2nd edn.)
5 IEEE Std. 519: IEEE Recommended Practices and Requirements for Harmonic Control in Electrical Power Systems', 1992
6 Singh, B., Gairola, S., Singh, B.N., Chandra, A., Al-Haddad, K.: 'Multipulse AC–DC converters for improving power quality: a review', *IEEE Trans. Power Electron.*, 2008, **23**, (1), pp. 260–281
7 Alves, R.L., Barbi, I.: 'Analysis and implementation of a hybrid high-power-factor three-phase unidirectional rectifier', *IEEE Trans. Power Electron.*, 2009, **24**, (3), pp. 632–640
8 Hartmann, M., Fehringer, R.: 'Active three-phase rectifier system using a 'flying' converter cell'. Proc. IEEE Advances in Energy Conversion Symp. ENERGYCON, Florence, Italy, September 2012, CD-ROM paper
9 Pejović, P.: 'Three-phase diode rectifiers with low harmonics–current injection methods' (Springer, 2007, 1st edn.)
10 Pejović, P., Janda, Ž.: 'Three-phase rectifiers that apply optimal current injection', *IEEE Trans. Aerosp. Electron. Syst.*, 2002, **38**, (1), pp. 163–173
11 Ivković, M., Pejović, P., Janda, Ž.: 'Application of optimal and suboptimal current injection in twelve-pulse three-phase diode rectifiers'. Power Electronics Specialists Conference, Rhodes, June 2008, pp. 3143–3149
12 Zhou, C., Ridley, R.B., Lee, F.C.: 'Design and analysis of a hysteresis boost power factor correction circuit'. Proc. IEEE Power Electronics Specialists Conference, PECS, Antonio, USA, June 1990, pp. 800–807
13 Singer, S.: 'The application of loss-free resistors in power processing circuits', *IEEE Trans. Power Electron.*, 1991, **6**, (4), pp. 595–600
14 Hansen, S., Enjeti, P.N., Hahn, J.H., Blaabjerg, F.: 'An integrated single-switch approach to improve harmonic performance of standard PWM adjustable-speed drives', *IEEE Trans. Ind. Electron.*, 2000, **36**, (4), pp. 1189–1196
15 Darijević, M., Pejović, P., Nishida, Y., Kolar, J.W.: 'Active resistance emulation in three-phase rectifier with suboptimal current injection'. Proc. Int. Symp. on Power Electronics, Novi Sad, Serbia, October 2011, CD-ROM paper
16 Pejović, P.: 'A novel low-harmonic three-phase rectifier', *IEEE Trans. Circuits Syst. I: Fundam. Theory Appl.*, 2002, **49**, (7), pp. 955–965
17 Maswood, A.I.: 'Unity power factor thyristor rectifier recent developments'. Int. Power Eng. Conf. IPEC, Singapore, November 2005, pp. 968–973
18 Vazquez, N., Rodriguez, H., Hernandez, C.: 'Three-phase rectifier applying active current injection', *IEEE Trans. Ind. Electron.*, 2009, **56**, (1), pp. 110–119
19 Janković, M., Darijević, M., Pejović, P., Kolar, J.W., Nishida, Y.: 'Hybrid three-phase rectifier with switched current injection device'. Proc. IEEE Power Electronics and Motion Control Conference PEMC, Novi Sad, Serbia, September 2012, CD-ROM paper
20 Božović, P., Pejović, P.: 'Current injection based low harmonic three-phase diode bridge rectifier operating in discontinuous conduction mode', *IEE Proc. – Electr. Power Appl.*, 2005, **152**, (2), pp. 199–208
21 Erikson, R.W., Maksimovic, D.: 'Fundamentals of power electronics' (Kluwer Academic Publishers, 2000, 2nd edn.)
22 Mohan, N., Undeland, T.M., Robbins, W.P.: 'Power electronics converters, applications and design' (Wiley, 2002, 2nd edn.)

doi: 10.1049/iet-pel.2013.0145